DIC-based monitoring on debonding crack propagation in wrapped composite joints

Feng, W.; He, P.; Koetsier, M.; Pavlovic, M.

Publication date
2022

Document Version
Final published version

Published in
Proceedings of the 20th European Conference on Composite Materials: Composites Meet Sustainability

Citation (APA)
Feng, W., He, P., Koetsier, M., & Pavlovic, M. (2022). DIC-based monitoring on debonding crack propagation in wrapped composite joints. In A. P. Vassilopoulos, & V. Michaud (Eds.), *Proceedings of the 20th European Conference on Composite Materials: Composites Meet Sustainability: Vol 1 – Materials* (pp. 1362-1368). EPFL Lausanne, Composite Construction Laboratory.

ECCM 20

26–30 JUNE 2022

LAUSANNE SWITZERLAND

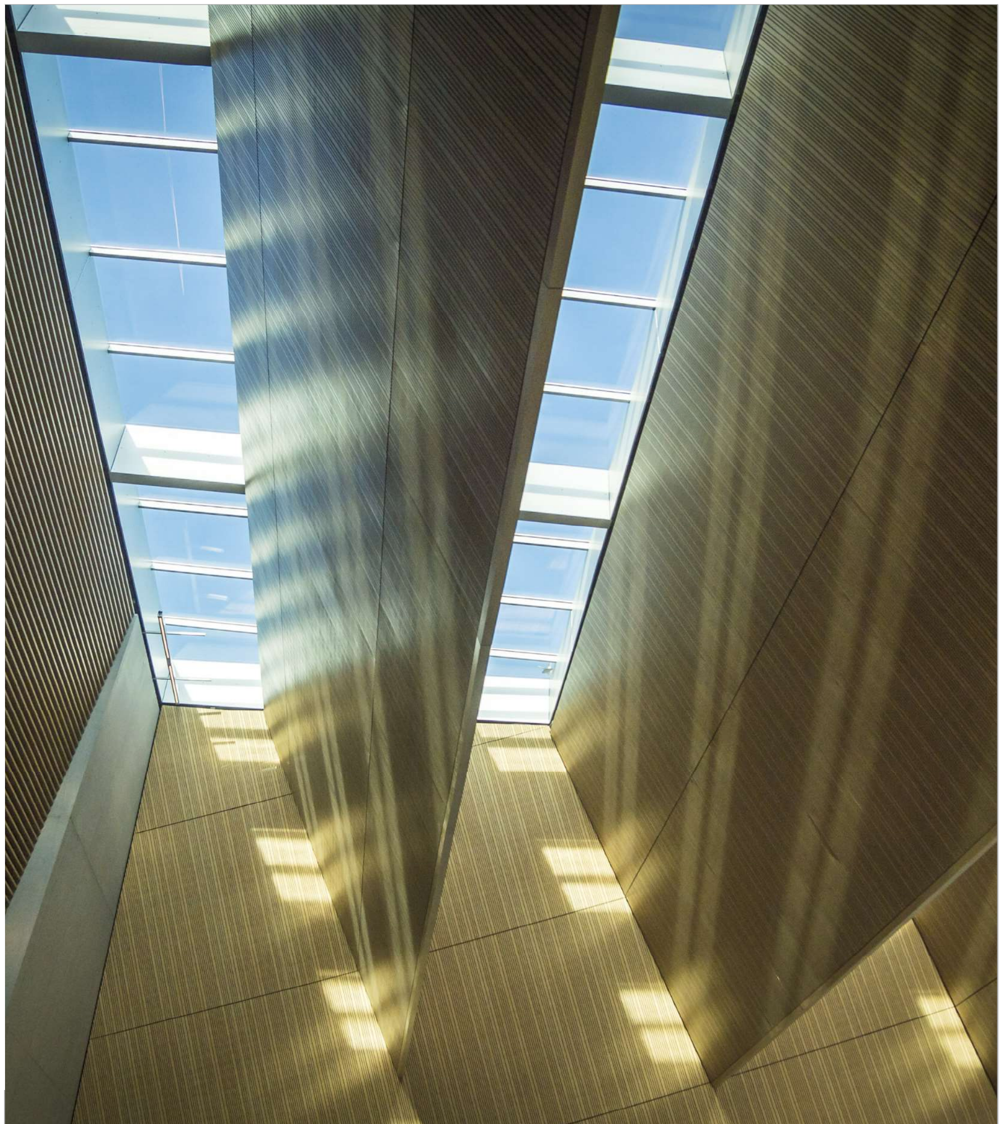

Proceedings of the 20th European Conference on Composite Materials

COMPOSITES MEET SUSTAINABILITY

Vol 1 – Materials

Editors : Anastasios P. Vassilopoulos, Véronique Michaud

Organized by :

EPFL

Under the patronage of :

CCLAB Composite Construction Laboratory

LPAC Laboratory for Processing of Advanced Composites

ESCM EUROPEAN SOCIETY FOR COMPOSITE MATERIALS

Proceedings of the 20th
European Conference on Composite Materials
ECCM20
26-30 June 2022,
EPFL Lausanne Switzerland

Edited By :

Prof. Anastasios P. Vassilopoulos, CCLab/EPFL
Prof. Véronique Michaud, LPAC/EPFL

Oragnized by:

Composite Construction Laboratory (CCLab)
Laboratory for Processing of Advanced Composites (LPAC)
Ecole Polytechnique Fédérale de Lausanne (EPFL)

ISBN: 978-2-9701614-0-0
DOI: http://dx.doi.org/10.5075/epfl-298799_978-2-9701614-0-0

Published by :

Composite Construction Laboratory (CCLab)
Ecole Polytechnique Fédérale de Lausanne (EPFL)
BP 2225 (Bâtiment BP), Station 16
1015, Lausanne, Switzerland

https://cclab.epfl.ch

Laboratory for Processing of Advanced Composites (LPAC)
Ecole Polytechnique Fédérale de Lausanne (EPFL)
MXG 139 (Bâtiment MXG), Station 12
1015, Lausanne, Switzerland

https://lpac.epfl.ch

Cover:

Swiss Tech Convention Center
© Edouard Venceslau - CompuWeb SA

Cover Design:

Composite Construction Laboratory (CCLab)
Ecole Polytechnique Fédérale de Lausanne (EPFL)
Lausanne, Switzerland

©2022 ECCM20/The publishers

Disclaimer:

DIC-BASED MONITORING ON DEBONDING CRACK PROPAGATION IN WRAPPED COMPOSITE JOINTS

Weikang, Feng[a], Pei He[a], Mathieu Koetsier[a], Marko Pavlovic[a]

a: Department of Engineering Structures, College of Civil Engineering and Geoscience, Technology University of Delft – w.feng@tudelft.nl

Abstract: *Wrapped composite joint is an innovative technique which connects steel hollow sections through bonding such that the fatigue performance is improved compared to welded joint. In this paper, a DIC-based method of monitoring surface strains is proposed to quantify the debonding crack propagation within the composite wrap layers during high cycle fatigue loading. A constant strain threshold was used to obtain crack length based on strain distribution curves extracted from DIC. Sensitivity analysis of such threshold showed that within the 'steady strain slope' region, the influence of threshold choice on calculated crack length is insignificant, but a good choice of threshold can help obtain more stable results. During cyclic loading, it was found that stiffness degradation and crack development of the joint is arrested due to friction effect at the cracked interface. Static tests after cyclic loading showed that the joint can still sustain its original static resistance.*

Keywords: Wrapped composite joints; Debonding crack propagation; Fatigue test; Digital Image Correlation

1. Introduction

Fatigue failure has been proved to be a common hazard for welded tubular joints, which are now widely used for circular hollow sections (CHS) of steel truss/jacket supporting structures of off-shore wind turbines, oil and gas platforms, steel bridges [1]. In recent years, fiber-reinforced polymers (FRP) have been widely used for enhancing static/fatigue performance of steel structures, due to their light weight, tailorability, high fatigue endurance and other excellent mechanical properties. In the previous study, an innovative joining technique, the wrapped composite joint was proposed by the authors [2], where composite wrap is used to connect steel members of hollow sections through bonding and welding can be completely avoided in the load transferring mechanism, and the low fatigue endurance due to welding is eliminated. Static [3] and fatigue [4] experiments on this kind of joints have shown their superior mechanical performance over their welded counterparts. However, monitoring the most important failure mode of the joint wrapped with thick laminates, debonding at the steel-to-composite interface still remains as a critical issue, which is of great importance for characterizing and predicting fatigue behaviour of wrapped composite joints.

During recent years, the non-destructive technique (NDT) has been widely used for mechanical damage assessment in composite structures [5], especially for monitoring debonding at composite-to-steel/concrete interface. Among these techniques, the Digital Image Correlation (DIC) technique has been widely used due to its advantages of non-contact, full field and real-time measurements. For example, Bahman Ghiassi [6], Pei Zhang [7] and Mohamad Ali-Ahmad [8] investigated debonding between FRP and substrates under quasi-static monotonic loads by DIC. Strain contours were captured under different load levels, where increased strains indicated crack initiation or debonding at the interface. The DIC method was also applied for investigating debond behaviour under fatigue loading [9]. The strain plateau along the CFRP plate represented the debond length which increased gradually with the increasing number of loading cycles. However, monitoring technique for debonding crack propagation at curved interface under thick laminates still needs to be developed.

In this paper, fatigue tests on axial wrapped composite joints were carried out. A 3D DIC system was utilized for capturing surface strain of the specimen such that debonding crack propagation at the composite-to-steel interface was monitored. A constant strain threshold was utilized to calculate crack length, meanwhile sensitivity of such threshold was conducted. After fatigue tests, static tests were carried out to determine the remaining static resistance of the joints.

2. Specimens, test set-up and loading protocol

Geometry and dimensions of specimens are shown in Figure 1. Two steel tubes of Φ60.3×4 with steel grade S355 are bonded together by composite wrap. The laminate of the composite wrap is formed with multi-directional composition of E-glass reinforcement and vinyl-ester based thermoset resin system. The composite wrapping thickness is $12mm$, while the total wrapping length is 480mm. A 25mm PTFE insert is applied at butt end of each tube forming 2 separate initial crack tips, such that the uncertainties related to crack initiation are reduced. A matt white paint was applied on the wrap, followed by a black speckle pattern to facilitate displacement and strain measurements using 3D DIC system. A total of 2 specimens were tested.

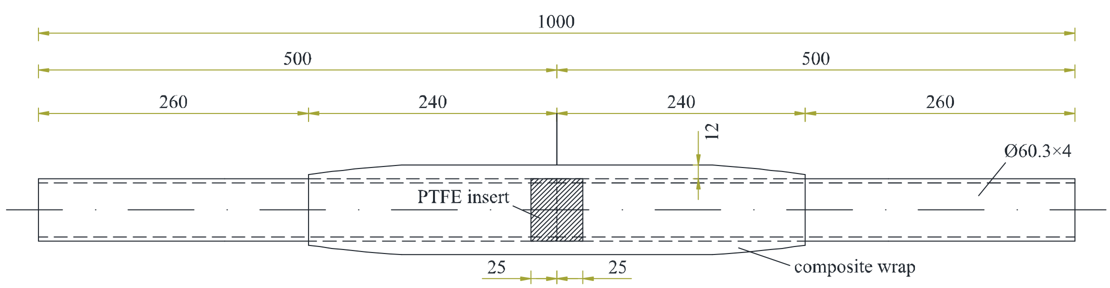

Figure 1. Geometry of specimen

Test set-up is shown in Figure 2. During the fatigue tests, all the specimens were loaded with the force range of 15-150kN (R=0.1), while the maximum force is approximately half of the static resistance obtained in separate tests. The loading frequency is 4Hz. Fatigue tests were stopped when stiffness degradation of the joint fully stabilized, then static tests were carried out on the same specimen to determine the remaining static resistance. The static tests were conducted through displacement control with the loading rate as 1mm/min. All the tests were carried out at room temperature.

GOM Aramis 3D DIC system with 12MPx cameras was positioned to acquire the local displacements and strains as shown in Figure 2. DIC measurement intervals during cyclic loading were controlled by the testing machine. At an interval of 1000 cycles, the cyclic loading is stopped, then photos are taken at the minimum and maximum forces, respectively.

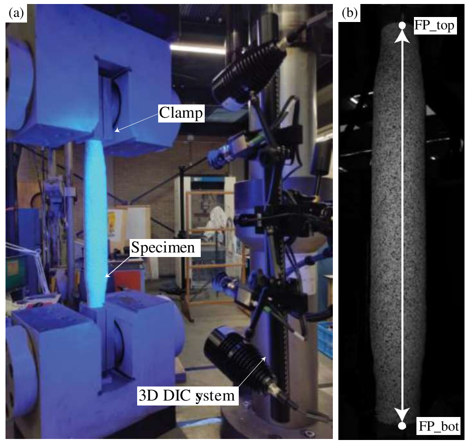

Figure 2. Test set-up and 3D DIC system

3. Test results and discussion

3.1 Stiffness degradation

To exclude any possible slip between the steel tube and grips of the testing machine at the load introduction point, the relative displacement, exclusively within the length of the specimen, measured by DIC technique was used to derive the stiffness degradation curves by Eq. (1).

$$k(N) = \frac{F_{max}(N) - F_{min}(N)}{\Delta L_{max}(N) - \Delta L_{min}(N)} \quad (1)$$

where $F_{max}(N)$ and $F_{min}(N)$ are the maximum and minimum applied forces at the Nth cycle, $\Delta L_{max}(N)$ and $\Delta L_{min}(N)$ are the elongations of the specimen between top and bottom facet points (see Figure 2 (b)) at the maximum and minimum loads respectively. Relative stiffness ($k(N)/k(1)$) against the number of cycles for both specimens are summarized in Figure 3. It can be seen from the figure that stiffness of the specimens degraded continuously during the cyclic loading due to crack propagation. It should be noted that the crack propagation can occur either as a debonding at the composite-to-steel interface or as an delamination within the composite wrap layers, which will be further discussed in section 3.2. Stiffness degradation shown in Figure 3 exhibits a stabilization trend for both tested specimens, namely a major (about 45%) stiffness degradation is found within the first 100,000 cycles, after which only 10% stiffness was lost until stop of the test at around 400,000 cycles. The stabilization phenomenon mainly results from stabilization of crack propagation, which will be discussed in section 3.3.

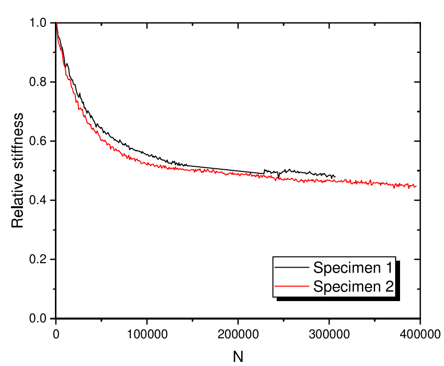

Figure 3. Stiffness degradation of specimens under fatigue load

3.2 Failure modes

During and after fatigue tests, no significant surface cracks were observed for both specimens. Further inspection was conducted through DIC system. Figure 4 (a) shows DIC contour plots of major principal strains on the surface of composite wrap corresponding to maximum loads at different cycles. It can be seen that the strain increased at the insert part at the first cycle. With increasing number of cycles, the strain-increased zone (in red colour) propagated steadily towards the wrapping ends. The increase of surface strains may be caused by multiple damage mechanisms, such as crack at the interface (debonding or delamination) and damage of the composite material. Considering the fact that the strain at the insert (middle) part, where force was only transferred by composite wrap, didn't increase so much during the cyclic loading shown in Figure 5, damage of the composite material can be neglected. Accordingly, the strain increase mainly reflected bonded interface crack propagation, which will be analysed quantitatively in the next section.

During the static test after cyclic loading, steel tubes were pulled out of the composite wrap for further inspection. It can be seen from Figure 4 (b) that there is still laminates remaining on the surface of steel tubes, indicating delamination occurring within the composite wrap layers.

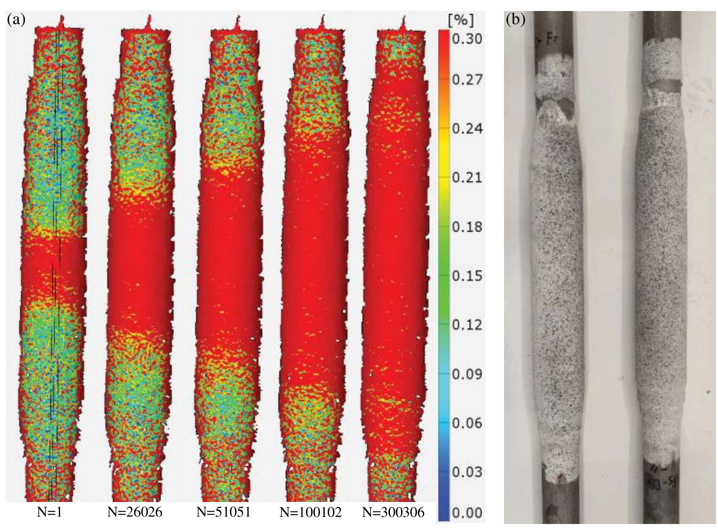

Figure 4. Failure modes of specimens (a) debonding crack propagation under cyclic loading; (b) steel tubes pulled out after static load

3.3 Debonding crack propagation

Strain distribution was extracted along the surface curves defined on the surface of composite wrap as shown in Figure 4 (a) for further analysis. The difference of strains at the maximum load and the minimum load was adopted here. The extracted strains at different number of cycles are plotted against distance to the middle of the joint in Figure 5. To average out some noise in the DIC strain measurements, the major strain was obtained along 3 surface curves and averaged. It shows that the strain is maximum in the middle, where there is the insert, and decreases gradually towards the wrapping ends. At the strain decreasing part, strain curves from different cycles are generally parallel to each other. Different from literature [9] which shows that there should be a strain plateau at the cracked part, the plateau is not obvious even at the insert part in the analysed case. This may be attributed to the shear deformation gradient of such thick composite laminates, which is caused by restraining from the bonded part and friction effect at the cracked interface. To avoid scatter of strain distribution at this area with complex stress state, a relatively low strain threshold was taken around the 'steady strain slope' region (between 0.1%-0.2%) to calculate the crack increments. The crack length is calculated separately for each brace and equals to the summation of crack increments each cycle plus the initial crack length of 25mm. A sensitivity analysis of the strain threshold was carried out as shown in Figure 5 (b). The results show that within the 'steady strain slope' region, the influence of adopting different thresholds is insignificant, while a higher or lower threshold may result in scattering of calculated results due to scattering of strain distribution curves outside the 'steady strain slope' region. In the following analysis, strain threshold of 0.15% is adopted for the analysed case.

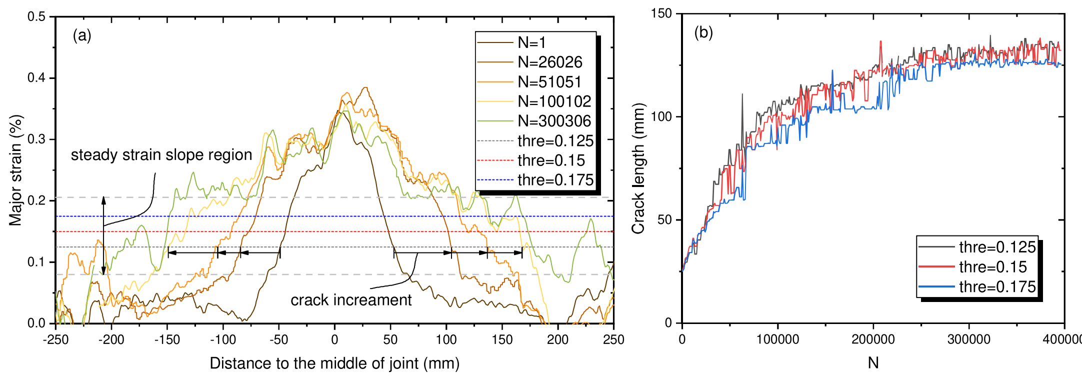

Figure 5. Crack length determination method (a) strain distribution along specimen (Specimen 2); (b) sensitivity analysis of thresholds for determining crack length (on bottom brace of Specimen 2)

The monitoring results for all the braces are summarized in Figure 6. It can be seen that for each specimen, crack propagations of top and bottom braces are identical, indicating symmetric fatigue performance of the specimens. Similarly to stiffness degradation, crack propagation rate also shows a stabilization trend. During the first 10,000 cycles, crack length increased steadily from 25mm to 115mm, while after that additional 15mm was achieved during the following 30,000 cycles leading to total crack length of 130mm. Considering that fatigue crack propagation is driven by strain energy release rate (SERR) at the crack tip according to Paris' law [10], this stabilization phenomenon is contradictory to the theory since the SERRs are constant at different crack lengths according to finite element analysis.

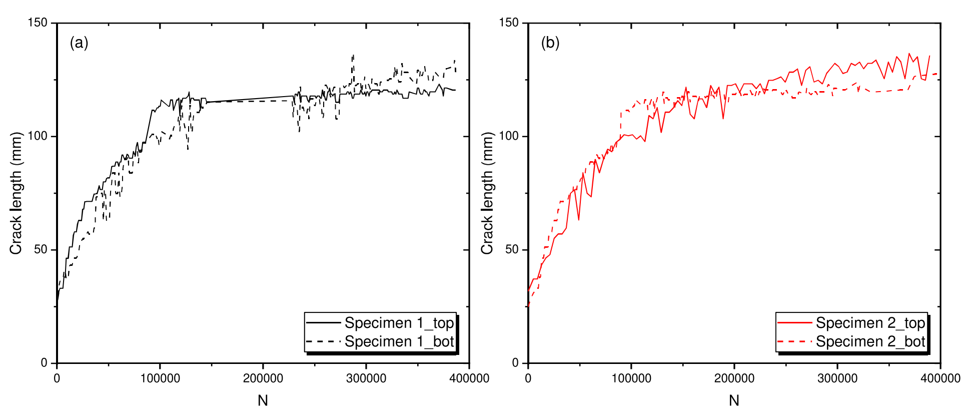

Figure 6. Crack growth on separate braces of (a) Specimen 1; (b) Specimen 2

An explanation can be made by looking at the failure mode given in Figure 4 (b), which is delamination within the first layer of composite wrap. The friction or fiber bridging effect at the cracked interface may dissipate part of the input energy, causing the SERR at the crack tip to reduce and leading to a smaller crack growth rate. Considering that fiber bridging effect is not predominate under mode II fatigue loading [11], the friction effect may dominate. This stabilization phenomenon is further studied out of the scope of this paper.

3.4 Static test after fatigue loading

After fatigue tests, the specimens were tested in monotonically increasing regime to check the influence of cyclic load on residual static resistance. The load-displacement curves are summarized in Figure 7. Results of specimens without being tested cyclically from previous study are also included for comparison. It can be seen that the initial stiffness of Specimen 1 and Specimen 2 is around 95kN/mm, which is 55% lower than that of previous specimens, namely 214kN/mm. This stiffness difference just equals to stiffness loss during cyclic load. After the elastic stage, a plateau due to steel yielding followed by hardening of steel materials was observed for Specimen 2 (The nominal yield strength of the steel tube is 252kN). The ultimate resistance of the specimen as well as the previous statically tested joint is around 300kN, after which a sudden failure occurred due to delamination as shown in Figure 4 (b). Considering that the remaining bond length for each braces is 240-130=110mm, the test results indicate that specimens with remaining bonding length of 1.5-2 diameters of the steel tube after cyclic loading can still sustain its original resistance. There is no sudden failure for Specimen 1, with the ultimate resistance being 260kN. After failure or ultimate resistance of the specimens, steel tubes were pulled out for further inspection which revealed that the failure plane is within the first layer of the composite laminate of the wrapped and not directly on the interface. This can be one explanation for steadily decreasing segment of the load-displacement curves.

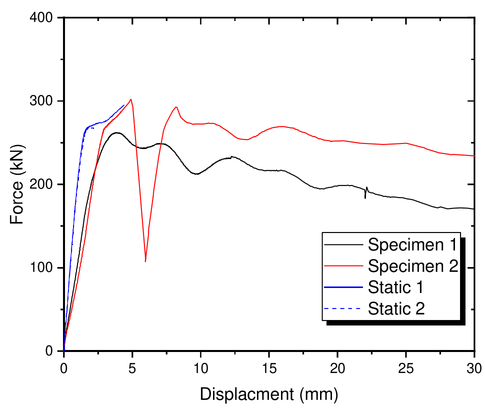

Figure 7. Load-displacement curve of specimens under static load after fatigue tests

4. Conclusions

Tensile fatigue tests were conducted on axial wrapped composite joints for 60mm diameter CHS steel tubes in this paper. 3D DIC system was employed to quantify the crack propagation within the specimen during cyclic load by monitoring surface strains on the composite wrap. A strain threshold was chosen after sensitivity analysis to determine the crack length. After fatigue tests, static tests were carried out to check the influence of cyclic load on residual static resistance of the joints. From studies mentioned above, main conclusions can be drawn as follows:

- Stiffness degradation of wrapped composite joints under cyclic loading is mainly due to delamination at the first composite wrap layer. The stiffness degradation exhibited a stabilization trend. A major stiffness degradation of 45% was found within the first 10,000 cycles, after which only 10% stiffness was lost in the remaining 390,000 cycles.
- Sensitivity analysis of strain threshold for determining crack length showed that the choice of threshold within the 'steady strain slope' region has insignificant influence on calculated crack length. A strain threshold of 0.15% was adopted in this study.
- After fatigue tests, the static resistance is the same with that of specimens without being tested cyclically.

Acknowledgements

The authors would like to express their gratitude to RVO for the financial support with Topsector Energiesubsidie van het Ministerie van Economische Zaken through WrapNode-I project. Acknowledgements are made towards GROW for their help in valorisation regarding renewable energy and energy transition and to Tree Composites B.V. for the production of specimens.

References

1. Wardenier J, Packer JA, Zhao XL, Van der Vegte GJ. Hollow sections in structural applications. Rotterdam, The Netherlands: Bouwen met staal. 2002.
2. Pavlovic M, Bogers P, Veljkovic M. Method for Making a Virgin Joint Between Two Separate Structural Hollow Sections. United States patent application US 17/052,303. 2021 Mar 18.
3. He P, Pavlovic M. Failure modes of bonded wrapped composite joints for steel circular hollow sections in ultimate load experiments. Engineering Structures 2022; 254:113799.
4. Feng W, Pavlovic M. Fatigue behaviour of non-welded wrapped composite joints for steel hollow sections in axial load experiments. Engineering Structures 2021; 249:113369.
5. Duchene P, Chaki S, Ayadi A, Krawczak P. A review of non-destructive techniques used for mechanical damage assessment in polymer composites. Journal of Materials Science 2018; 53:7915-38.
6. Ghiassi B, Xavier J, Oliveira D V., Lourenço PB. Application of digital image correlation in investigating the bond between FRP and masonry. Composite Structures 2013; 106:340-9.
7. Zhang P, Lei D, Ren Q, He J, Shen H, Yang Z. Experimental and numerical investigation of debonding process of the FRP plate-concrete interface. Construction and Building Materials 2020; 235: 117457.
8. Ali-Ahmad M, Subramaniam K, Ghosn M. Experimental Investigation and Fracture Analysis of Debonding between Concrete and FRP Sheets. Journal of Engineering Mechanics 2006; 132:914-23.
9. Wang HT, Wu G, Pang YY, Shi JW, Zakari HM. Experimental study on the bond behavior between CFRP plates and steel substrates under fatigue loading. Composites Part B 2019; 176:107266.
10. Anderson WE, McEvily AJ. A Critical Analysis of Crack Propagation Laws. Journal of Basic Engineering 1963; 85(4): 528-533.
11. Khan R. Fiber bridging in composite laminates: A literature review. Composite Structures 2019; 229:111418.